ELSEVIER

Physica B 230–232 (1997) 313–316

PHYSICA B

The structural, magnetic and transport properties of $Pr_{0.6}(Ca_{1-x}Sr_x)_{0.4}MnO_3$

M.R. Lees[a,*], L.J. Chang[a], J. Barratt[a], G. Balakrishnan[a], C.V. Tomy[a], D. McK. Paul[a], C.D. Dewhurst[b], C. Ritter[c]

[a]*Physics Department, University of Warwick, Coventry, CV4 7AL, UK*
[b]*IRC in Superconductivity, University of Cambridge, Cambridge CB3 0HE, UK*
[c]*Institut Laue Langevin, BP 156, F-38042 Grenoble Cedex 9, France*

Abstract

Transport and magnetic measurements as a function of both temperature and magnetic field as well as neutron powder diffraction studies have been used to investigate the properties of $Pr_{0.6}(Ca_{1-x}Sr_x)_{0.4}MnO_3$ ($0 \leqslant x \leqslant 1$) as a function of x. This system exhibits a remarkable sensitivity to changes in x, underlining the strong correlation between the structural, magnetic and electronic properties of the manganite materials.

Keywords: $Pr_{0.6}(Ca_{1-x}Sr_x)_{0.4}MnO_3$; Magnetoresistance

Perovskites of composition $R_{1-x}A_xMnO_3$ (R = rare earth and A = alkaline earth) have attracted considerable interest because they display a range of extraordinary magnetic, electronic and structural properties. Here we concentrate on materials with the composition $Pr_{0.6}(Ca_{1-x}Sr_x)_{0.4}MnO_3$ $(0 \leqslant x \leqslant 1)$ [1–4]. Transport and magnetic measurements as a function of both temperature, T and magnetic field, H, as well as neutron powder diffraction studies have been used to investigate the evolution of the properties of this series of compounds as a function of Ca concentration. Although the level of alkaline earth doping remains constant throughout the series, the compounds are shown to exhibit very different properties. The observed changes in the structure have been correlated with the changes in the nature of the magnetic ordering and the electronic properties of this system.

* Corresponding author.

Polycrystalline samples of $Pr_{0.6}(Ca_{1-x}Sr_x)_{0.4}MnO_3$ ($0 \leqslant x \leqslant 1$) were prepared using stoichiometric quantities of Pr_6O_{11}, $CaCO_3$, $SrCO_3$ and MnO_2. These materials were repeatedly ground and sintered in air for 12 h at 1350°C before finally being pressed into pellets and sintered at 1350°C for 24 h.

Fig. 1 presents χ_{AC}-T data for selected samples. For $x \leqslant 0.15$, a peak around $T_{CO} = 250$ K indicates a structural/charge ordering (CO) transition. A feature at $T_N \approx 170$ K marks the transition to an antiferromagnetic (AFM) state. The peak at low T may be due to a spin reorientation [1, 5]. For $0.15 \leqslant x \leqslant 0.25$ there appears to be a coexistence of AFM and ferromagnetic (FM) ordering. For $0.25 \leqslant x \leqslant 1.0$ the system is FM with rapid increase in the Curie temperature, T_c, with x. The increasingly T-dependent response below T_c suggests the system is becoming more anisotropic.

Neutron diffraction data confirms this picture. For $x = 0.0$, the change in half width of several nuclear lines at $T \approx 250$ K indicates the structural/

PII S0921-4526(96)00698-9

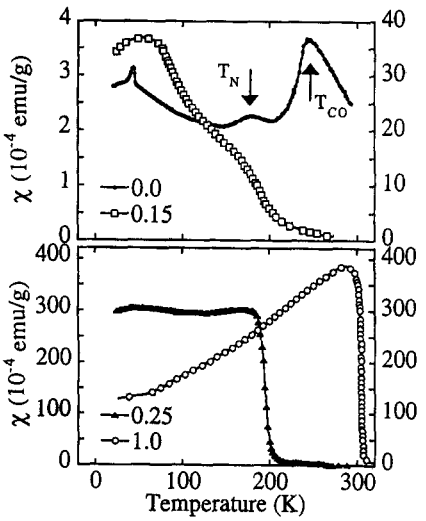

Fig. 1. Temperature dependence of AC susceptibility for selected $Pr_{0.6}(Ca_{1-x}Sr_x)_{0.4}MnO_3$ samples. Open symbols refer to right-hand scale, closed symbols refer to left-hand side.

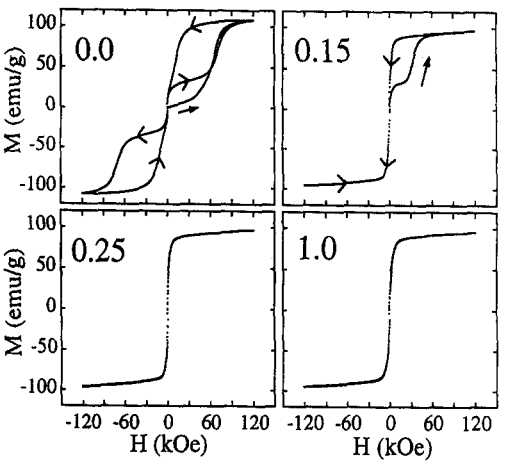

Fig. 2. Magnetisation versus field curves taken on samples cooled in zero field to 10 K. Solid arrows indicate data collected during initial field sweep.

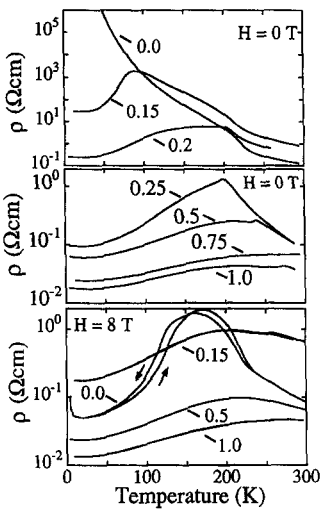

Fig. 3. Resistivity versus temperature data collected in magnetic field of 0 and 8 T for some $Pr_{0.6}(Ca_{1-x}Sr_x)_{0.4}MnO_3$ samples.

CO transition. Below 170 K additional magnetic Bragg peaks indicate AFM order. The system has a CE structure with two magnetic sublattices of Mn atoms where $\mu_{AF1} = 2.75\mu_B$ and $\mu_{AF2} = 2.72\mu_B$ [3,5]. For $0.06 \leqslant x \leqslant 0.25$ the materials have a similar AFM structure with an additional FM component. For $0.25 \leqslant x \leqslant 1.0$ the system has a simple FM structure with a moment $\mu_{FM} \approx 3.3\mu_B$. The T_c's deduced from neutron data agree well with those extracted from χ_{ac}-T measurements. For $x \approx 1.0$ there is a low T structural transition to a monoclinic I2/a phase [5].

Magnetisation, M, versus H curves have been taken in order to study the H dependence of the magnetic ordering (see Fig. 2). For $x \leqslant 0.15$, the application of a sufficiently intense field at $T \leqslant T_{CO}$ produces a metamagnetic transition to a FM state. At $T \leqslant 50$ K there is an irreversible change in the response after the initial field sweep. As x increases the metamagnetic transition occurs at lower H [1,2]. For $x \geqslant 0.25$ the curves resemble those of soft FM systems. The saturation moments are close to the spin only values expected for the Mn^{3+}/Mn^{4+} ratio present in these materials.

Transport measurements have been made in order to study the nature of the conduction mechanism. Fig. 3 shows resistivity, ρ, versus T curves taken in different H. The Ca-rich compounds exhibit activated behaviour in zero H. The data can be fitted using $\rho = \rho_0 \exp(T_0/T)^p$, where T_0 is some effective temperature. Reasonable fits have been obtained for $p = 1$ (nearest-neighbour hopping) and $p = \frac{1}{4}$ (3D Mott hopping), consistent with polaronic conductivity [6]. For $x = 0$, the activation energy at high T, calculated using $p = 1$ is around

0.06 eV. The change in the slope of ρ–T below 250 K is associated with the structural/CO transition and indicates an increase in the activation energy. For $H \geqslant 4T$, there is a maximum in ρ–T which shifts to higher T with increasing H. There is low T minimum and considerable hysteresis in the data. The magnetoresistance, $MR = \Delta R/R_H$ where $\Delta R = (R_H - R_0)$ exceeds 10^9% in 8T at 5 K (see Fig. 4). The ρ–T curves of the FM samples have a zero field maximum around T_c. Below T_c, the behaviour is unlike that of conventional metal. ρ decreases with T, but cannot be fitted to any well-accepted power low, whilst at low T, ρ increases. The overall magnitude of the MR decreases and the T at which the MR is a maximum increases (see Fig. 4). There is little hysteresis in the data.

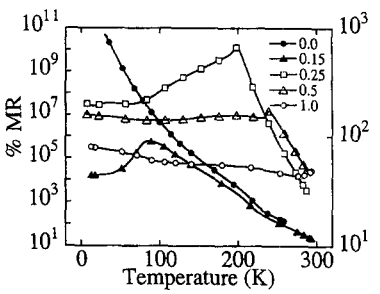

Fig. 4. Variation of magnetoresistance with temperature for selected $Pr_{0.6}(Ca_{1-x}Sr_x)_{0.4}MnO_3$ samples. (open symbols refer to right-hand scale, closed symbols refer to left-hand scale).

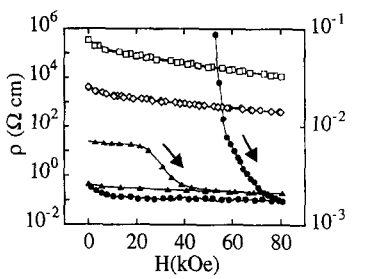

Fig. 5. Resistivity versus magnetic field data taken at 10 K on ZFC samples of $Pr_{0.6}(Ca_{1-x}Sr_x)_{0.4}MnO_3$ where $x = 0.0$ (●), $x = 0.15$ (▲), $x = 0.25$ (□) and $x = 1.0$ (◇). Arrows indicate data collected with increasing H (open symbols refer to right-hand scale, closed symbols refer to left-hand scale).

Fig. 5 shows ρ–H curves for selected samples. For $x \leqslant 0.25$, the ZFC samples exhibit a transition from an insulating to a conducting state as H increases. This change in ρ correlates with the metamagnetic transition discussed above. At low T, this conducting state is metastable, with the samples remaining conducting when H is reduced to zero. At higher T there is considerable hysteresis in the ρ–H data, but ρ returns to its original value in zero field. The field required to induce a conducting state decreases with increasing x.

Fig. 6 shows the thermopower, S, versus T, for several values of x. For Ca rich samples, the TEP at high T is -20 ± 5 μV/K, cf. -25 μV/K calculated using the small polaron formula $S(T) = -(k_B/|e|[\beta c/(1-c)]$ where c is Mn^{4+}/Mn ratio and β (= 2) is the spin degeneracy [6]. The rapid increase in S–T below 250 K can be attributed to trapping out of some mobile carriers at $T < T_{CO}$. As x increases, the feature around 250 K becomes less evident. In addition, the magnitude of S at high T and the overall change in S with T are substantially reduced. For $x = 1.0$ the data can be well fitted using $S(T) = AT + BT^3$ where the two terms refer to the diffusion and the phonon drag contributions to the TEP, respectively.

The properties of $Pr_{0.6}(Ca_{1-x}Sr_x)_{0.4}MnO_3$ show remarkable sensitivity to changes in x, highlighting the strong correlation between the structura, magnetic and electronic properties of these manganite materials. At 300 K the samples have an orthorhombic Pnma structure. Distortions are introduced by a combination of the mismatch

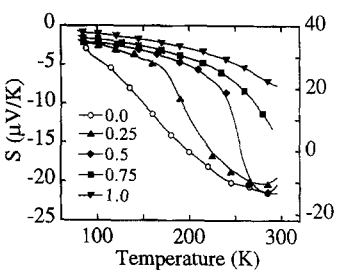

Fig. 6. Thermopower versus temperature for several values of x (open symbols refer to right-hand scale, closed symbols refer to left-hand scale).

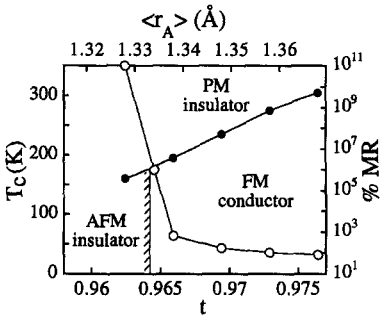

Fig. 7. Transition temperature (●) and magnetoresistance (○) versus t (or $\langle r_A \rangle$) for the $Pr_{0.6}(Ca_{1-x}Sr_x)_{0.4}MnO_3$ ($0 \leqslant x \leqslant 1$) system.

in the size of the alkaline earth atom and the dynamic Jahn–Teller effect. The tolerance factor $t = (R\text{–}O)/\sqrt{2}(A\text{–}O)$ (where R–O and A–O are the equilibrium bond lengths) gives measure of the degree of distortion present. Using the values for ionic radii in 12-fold coordination gives $t = 0.96$ for $x = 0.0$. This is close to the critical value delineating the boundary between AFM/insulator and FM/conductor. The application of magnetic field can drive the material FM. Once in the FM state, the increased mobility of the charge carriers leads to a fall in ρ producing an insulator–metal transition and the large MR seen at low T. t increases with addition of Sr. This leads to a stronger double exchange mediated FM coupling. There is a strong correlation between t (or $\langle r_A \rangle$) and T_c (see Fig. 7). In the FM state the decrease in ρ in zero H leads to an overall decrease in MR. The maximum MR is observed around T_c with an unusual conducting state at $T < T_c$.

References

[1] M.R. Lees, J. Barratt, G. Balakrishnan, D. McK, Paul and M. Yethiraj, Phys. Rev. B 52 (1995) 14903; M.R. Lees, J. Barratt, G. Balakrishnan, D. McK. Paul and C.D. Dewurst, J. Phys.: Condens. Matter 8 (1996) 2967.

[2] H. Yoshizawa, H. Kawano, Y. Tomioka and Y. Tokura Phys. Rev. B 52 (1995) 13 145; Y. Tomioka, A. Asamitsu, Y. Moritomo and Y. Tokura J. Phys. Soc. Japan 64 (1995) 3626.

[3] Z. Jirak, S. Vratislav and J. Zajicek, Phys. Stat. Sol. 52 (1979) 39; E. Pollert, S. Krupicka and E. Kumzicova, J. Phys. Chem. Solids 43 (1982) 1137; Z. Jirak, S. Krupicka, Z. Simsa, M. Dlouha and S. Vratislav, J. Magn. Magn. Mater. 53 (1985) 153.

[4] A. Maignan, Ch. Simon, V. Caignaert and B. Raveau B, Solid State Commun. 96 (1995) 623; B. Raveau, A. Maignan and V. Caignaert, J. Solids State Chem. 117 (1995) 424.

[5] C. Ritter, P. Radaelli, M.R. Lees, J. Barratt, G. Balakrishnan, D. McK. Paul, J. Solid State Chem., to be published.

[6] N.F. Mott, Metal–Insulator Transition (Taylor & Francis, London, 1974; 2nd ed).